PCCP

Accepted Manuscript

ROYAL SOCIETY OF CHEMISTRY

www.rsc.org/pccp

Reaction between HN and SN: A possible channel for the interstellar formation of N_2 and SH in the cold interstellar clouds.

Authors: Priya Bhasi, Zanele P. Nhlabatsi, Sanyasi Sitha*

Department of Chemistry, University of Johannesburg, PO Box 524, Auckland Park, Johannesburg, South Africa 2006

Abstract: Using computational calculations potential energy surface (PES) of the reaction between NH and NS has been analysed. The PES of the reaction shows the formation of two very stable species, HNSN and HNNS. Out of these two, HNNS which has the signature N-N linkage was found to be the most stable species in the PES. In view of the highly exothermic nature of the reaction surface, it has been proposed that these two species can possibly be detected in the interstellar space. For the first time it has also been shown that the reaction between the NH and NS can lead to the possible formation of N_2 via the isomer HNNS, and how the effect of tunnelling can make this reaction very much feasible, even in the extreme low temperature conditions prevailing in the interstellar medium. Based on already reported results, similar kind of behaviour for the NH + NO reaction surface has also been proposed. These dissociation reactions leading to the formation of N_2 can be considered as potential secondary contributing channels while accounting for the total estimates of the N_2 in the interstellar medium, and thus HNNS as well as HNNO can be considered as stable reservoir molecules for interstellar N_2. Besides the formation of N_2, formation of another astronomically important radical, SH in the cold interstellar clouds has also be proposed.

*To whom correspondence should be addressed: Email: ssitha@uj.ac.za

Key Words: Interstellar Medium, ISM, N_2, HNNS, HNSN, NH, NS, NO

1. Introduction:

Nitrogen is one of the most abundant elements in the universe and also one of the essential elements to produce many prebiotic organic molecules/precursors in the interstellar medium (ISM). As of today, almost 70 species have been detected in ISM which contains one or more nitrogen atom(s) in their skeletons[1-10]. This gives a clear indication that nitrogen bearing molecules are very much crucial in understanding the active chemistry existing in the ISM[11-20]. The detection as well as the estimation of the abundance of molecular form of nitrogen; N_2 in the ISM has been particularly problematic and this is due to the fact that N_2 is a symmetric diatomic molecule, without a dipole moment. Due to this lack of a dipole moment, detection of N_2 relies on its electronic transitions in the far-ultraviolet region, which is inaccessible for earth based telescopes[21]. Till date the only reported direct measurement of N_2 in the diffuse interstellar clouds, in the far-ultraviolet wavelength range is by knauth et al., where the low column densities of the diffuse interstellar clouds permit the light to pass and a star along the line of visualization was used to probe the species in the interior.[22] Beside this only direct measurement, there exist many indirect measurements mostly via the measurements of the N_2H^+ and its deuterated forms[17,18,21,23-27]. Formation of molecular N_2 largely affects the elemental nitrogen partitioning and subsequently the related nitrogen chemistry as N_2 is a highly stable molecule with very large bond dissociation energy[21]. Formation of N_2 in the dense interstellar clouds is believed to be by two pathways (as shown below), where atomic nitrogen is the initiator of the reaction channel for both the paths[11,21].

Pathway 1:

$N + OH – NO + H$

$N + NO – N_2 + O$

Pathway 2:

$N + CH – CN + H$

$N + CN – N_2 + C$

Besides these proposed two paths, are there any other paths which can contribute to the total N_2 content of the ISM and thus can affect the elemental nitrogen partitioning? In other words are there any other reactions which can produce N_2 in the ISM, from the interactions of nitrogen containing molecules/fragments already detected in the ISM? A search has been carried out to find some simple (diatomic) N-atom containing molecules/fragments already detected in the ISM and found the species like CN, NH, NO, NS, PN and SiN[1]. These species when interact with each other, they are capable of producing molecules with signature N-N linkage[28]. The importance of these kinds of molecules with signature N-N linkage is that if they dissociate, they are capable of producing N_2 and thus will be able to enrich the amount of interstellar N_2. Thus, these kinds of molecules can be viewed as potential reservoir molecules for N_2 in the interstellar medium. One such interesting species is HNNO (or even its other isomer, HONN) formed from the reaction of NH with NO, and is the focus of the recent study carried out by Peterson et al.[28]. Even the cationic forms of the HNNO system, like $HNNO^+$, NNOH+ have been well studied in great details.[29,30] Also, there exist many more studies, both computational as well as experimental for the reaction of NH with NO[31-38]. The analogue molecule to HNNO is the HNNS, which has not been discussed anywhere in the literature. This is in spite of the fact that the breeding fragments like, NH and NS (sulphur analogue of NO) are readily available in the interstellar medium[39-43]. Keeping eye on the importance of these kinds of molecules and availability of the fragments like, HN and NS in the ISM, for the first time we have carried out a detailed potential energy surface (PES) analysis for [H,N,N,S] using computational calculations. Besides the formation of isomers, we have also discussed the dissociation channels from various isomers, to know if they can lead to the formation of N_2 and possibly can enrich the N_2 content of the ISM. Also, wherever possible, we have compared our results with the NH + NO reaction surface.

2. Computational methods:

All quantum-chemical calculations have been performed using Gaussian 09 package and the geometries of all the stationary points in the PES have been visualized using GaussView program.[44] In this work, all DFT (density functional theory) calculations were performed by using the B3LYP exchange–correlation functionalities theoretical level,[45,46] using 6-31++G(3df,2pd) basis set, unless otherwise mentioned. Optimizations of the open-shell species have been carried out using UHF methodology[47] and for closed-shell species, RHF methodology was used. For the shake of comparison, MP2 calculations[48,49] were also performed using same basis functions. Harmonic vibrational frequencies were computed to evaluate the zero-point vibrational energy (ZPVE) corrections, which have been included in all the reported energies in this work. It is notable that no imaginary frequencies were found for all the isomers, reactants and the complex; which verify that they were all minima in the PES at all of the theoretical levels investigated in this work. The basisset superposition error (BSSE), a source of error in supermolecular calculations happens due to the finite size of the basissets. For accurate treatments, this error has been accounted for by the counterpoise correction of Boys and Bernardi[50]. Transition states were confirmed from the analysis of their frequencies, by ensuring that only one imaginary frequency for each of those transition states. We have also carried out analysis of the displacement vectors for the imaginary frequencies of those transition states, to ascertain that the transition states were structurally true transition states, and also confirmed them from their IRC (intrinsic reaction coordinates) analysis[51]. It was found that MP2 and B3LYP methods both predict similar kinds of trends for the PES, thus discussion reported in this work are limited only to the B3LYP method, and the results related to MP2 method are provided in the supporting information (also results related to G3B3 method[52], a composite method used for accurately calculate the energies, are provided in the supporting information). To account for the dispersive and long-range interactions in the DFT methods, for some of the transition states and for the pre-reaction complex, calculations have been carried out using wB97XD method.[53] Incorporation of these corrections was very much crucial in view of the nature of interaction existing in this reaction PES.

3. Results and discussions:

3.1. Isomers:

With the thorough analysis nine stable isomers have been located in the PES. All these nine isomers are shown in Figure 1. Out of these nine isomers, four isomers have chain like structures, two have cyclic structures and three are branched chain structures. Analysis of the four chain isomers, i.e., isomers 1-4, shows that isomers 1 and 2 have the linkage as H-N-S-N, and isomers 3 and 4 have the linkage as H-N-N-S. In the two cyclic isomers, i.e., isomers 5 and 6, central to their structures is a three membered cyclic ring; cyclic N-N-S linkage. In both the isomers the H-atom is out of plane and almost perpendicular to the plane of N-N-S ring. The remaining three isomers, i.e., isomers 7, 8 and 9 have branched chain structures. Isomers 8 and 9 are structurally similar, but geometrically slightly different. The major differences are due to the bond angles arising as consequence of the nature of bonding. In the isomer 8, the NSN bond angle is 141.6°, whereas for the isomer 9 this bond angle is 155.5°. Comparison of the geometries of these nine isomers obtained from the B3LYP method and MP2 method shows that they are structurally very similar.

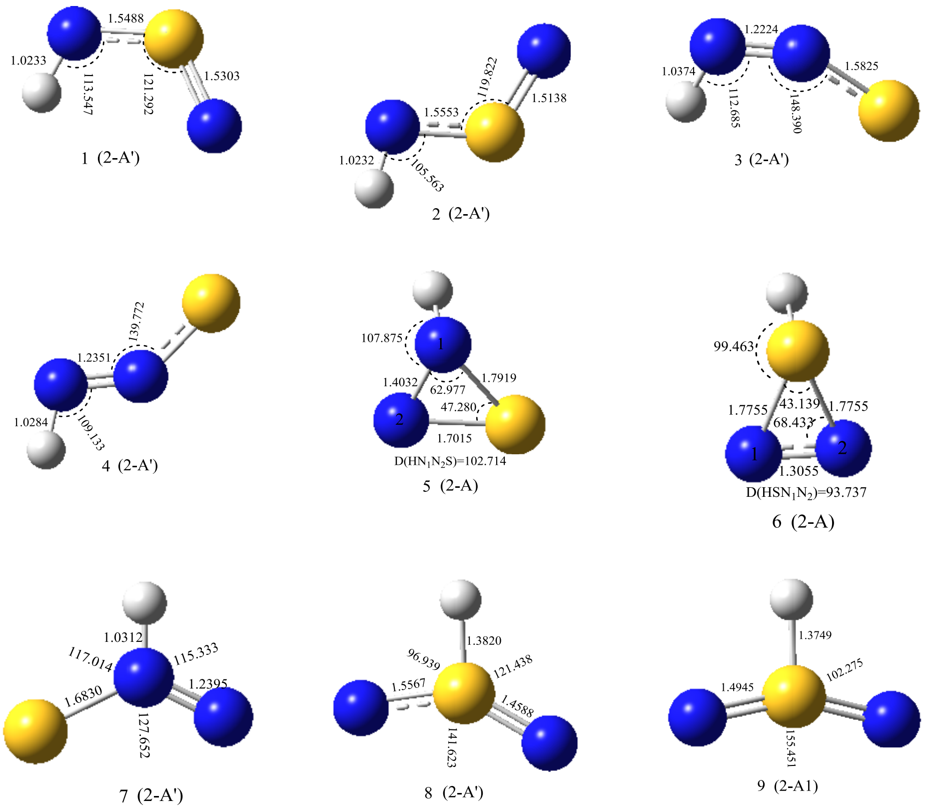

Figure 1: B3LYP/6-31++G(3df,2pd) optimized geometries of the isomers. Bond lengths are in angstroms and bond angles are in degrees.

Besides these nine isomers a pre-reaction complex has also been located in the PES. This complex (C) is shown in Figure 2. Analysis of the pre-reaction complex shows that all the four atoms are arranged in a straight line (co-linear arrangement) and are on the C_{∞} molecular axis.

The major parameter is the distance between (S)N – H(N) and is 2.383 Å (MP2 method also predict similar geometry like that of B3LYP method, where this distance is 2.321 Å). This gives a clear indication that the complex formation is due to the hydrogen bonded interaction between the H-atom of the HN with the N-atom of the SN. To have an idea about the nature of interaction existing in this complex, electrostatic potential (ESP) maps of the reactants SN and HN have been calculated and visualized. The ESP maps of the reactants are also shown in Figure 2. Analysis of the ESPs shows that, for NS there are negative potentials around N-atom and positive potentials around the S-atom; whereas for NH the negative potentials are found to be around the N-atom and positive potentials are found to be around the H-atom. Fitting these ESP maps of the reactants in the complex geometry, one can say that the nature of interaction existing in the complex is electrostatically a favourable one. Also, the ESP maps clarifies that though the complex has a linear structural arrangement, it is not due to σ-hole interactions, rather the complex can be treated as a hydrogen bonded complex.

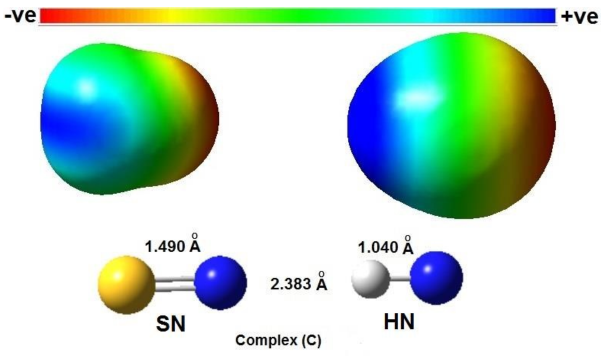

Figure 2: B3LYP/6-31++G(3df,2pd) optimized geometries of the complex (bottom). In the top computed ESP maps of SN and HN (oriented in the similar fashion like that of the complex) calculated from the B3LYP/6-31++G (3df,2pd) method using 0.001 au electron density surfaces.

3.2. Transition states:

Thirteen transition states (TS) in the PES have been located in the PES and are shown in Figure 3. Out of these thirteen TSs, ten are related to isomerization transition states between various isomers, one is related to reaction between NH and NS at the entry channel of the reaction, and two are dissociation transition states leading to the formation of the most important fragments N_2 and SH.

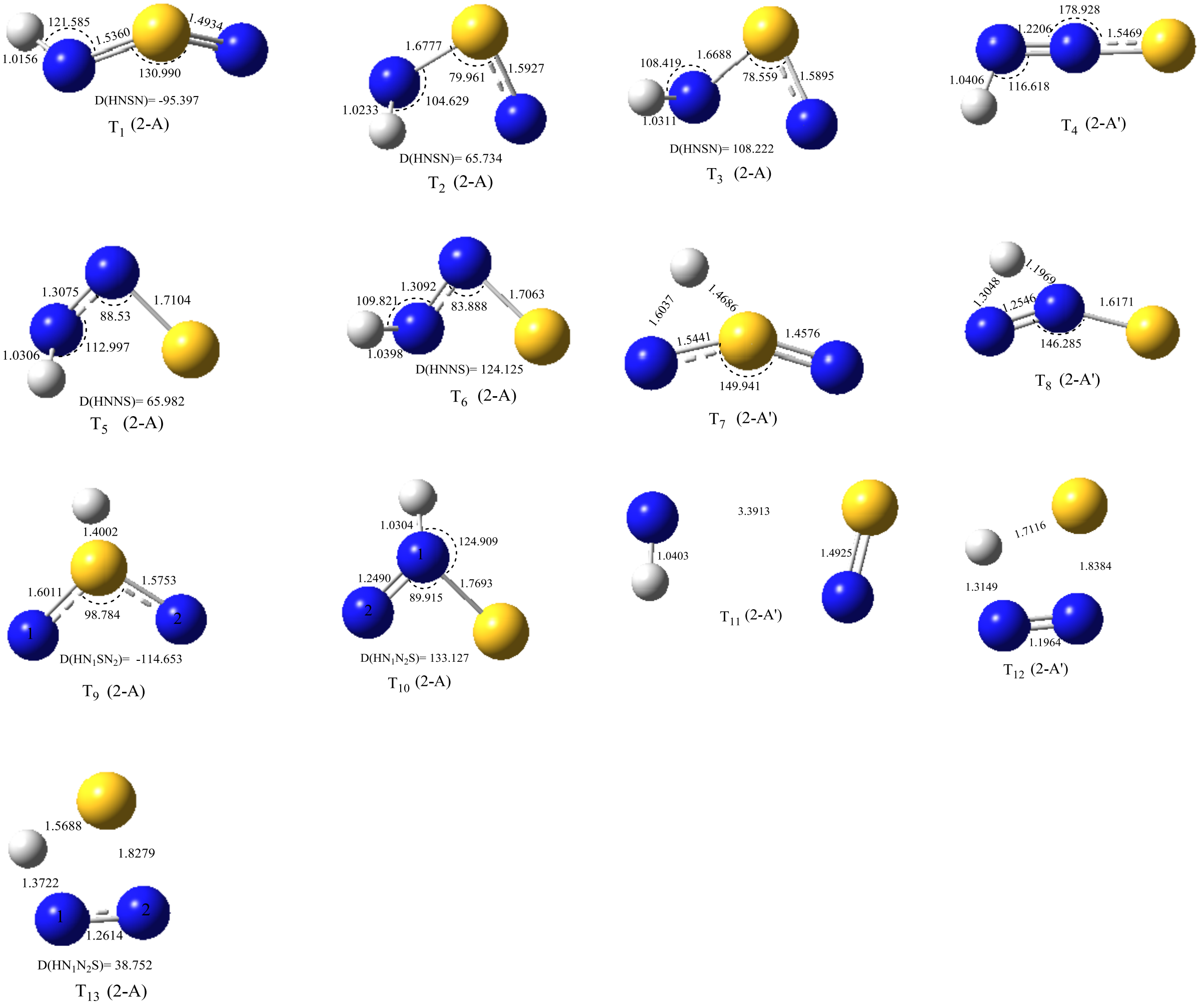

Figure 3: B3LYP/6-31++G(3df,2pd) optimized geometries of the transition states. Bond lengths are in angstroms and bond angles are in degrees.

<u>Nature of interactions in the TSs and long-range dispersion corrections:</u> Use of the DFT based methods (like, B3LYP, even G3B3 which uses the B3LYP optimized geometry of the system for higher energy corrections) resulted in three association transition states or reaction transition states (T_{11} in Figure 3, and the other two, ST_1 and ST_2 provided in the supporting information) for the reaction between NH and NS. Analysis of these three transition states shows that, ST_1 leads to the formation of the isomer 4, ST_2 lead to the formation of isomer 3 and T_{11} lead to the formation of isomer 1. But, on the other hand when some non DFT based methods (like MP2 which correctly accounts for the dispersive forces) were employed, no transition states have been found. When B3LYP optimized transition state geometries for ST_1 and ST_2 (supporting information) were used as the starting geometries for the MP2 optimizations, in the obtained optimized structures the reactants HN and NS got separated to a larger distances. On the other hand when the B3LYP optimized geometry of T_{11} was used as the starting geometry for the MP2 optimization, the structure of the TS remain almost intact, but it showed two imaginary frequencies. To account for the reason for this behaviour we used the ESP maps of the reactants, NH and NS (shown in Figure 2) to study the nature of interactions existing in these three TSs obtained in the B3LYP method. When the ESP maps of the reactants, NH and NS were fitted on the geometric arrangements of the ST_1 and ST_2 (Supporting information), it was found that the interactions were electrostatically unfavourable, and this is due to the fact that negative electrostatic potentials of N-atom of NH and N-atom of NS were in close proximity. On the other hand in the case of other reaction transition state T_{11}, arranging the reactant ESP maps according to the TS geometry, favourable interactions have been found between the positive potentials of the S-atom of the NS with the negative potentials of the N-atom of the NH, and negative potentials of the N-atom of the NS with the positive potentials of the H-atom of the NH. In this case the two fragments are separated by a large distance to avoid the repulsive interactions between the positive potentials of the S-atom and H-atom, and the negative potentials of the N-atoms of both fragments.

In view of the nature of electrostatic interactions existing in these three transition states, it is definitely crucial to take into account the dispersion forces by considering the long range interactions. To account for this, calculations have been carried out using the wB97XD method which includes the empirical dispersion as well as long range corrections[52]. Incorporating the dispersion as well long range interaction corrections into the DFT method, only one reaction transition state, T_{11} was found to be existing in the PES. wB97XD method also indicated the nonexistence of the other two transition states ST1 and ST2, like that of the MP2 method. As discussed earlier, in the cases of ST_1 and ST_2, where the arrangements of the reactants are electrostatically unfavourable (more repulsive), inclusion of the long range dispersion corrections might have destabilised the transition states further. Thus when these two transition states were reinvestigated using the long range dispersion corrections, starting from their respective B3LYP optimized geometries, they were no more identified as transition states (rather showed situations where in both the obtained geometries, reactants were found to be separated by very large distances). On the other hand for T_{11} where the interactions were electrostatically favourable, calculations incorporating the long-range dispersion corrections resulted in the same transition state. This gives a very clear indication that while dealing with these kinds of systems, one need to be very cautious, and inclusion of long-range dispersion corrections might play a decisive role. Geometries of this transition state obtained using the wB97XD method is also provided in the supporting information, and the related energetics is discussed in the section 3.4. The isomerization transition states and the dissociation transition states are discussed in sections 3.3 and 3.4 respectively.

3.3. Potential Energy Surface:

Computed potential energy surface for the reaction between NH and NS using B3LYP method is shown in the Figure 4.

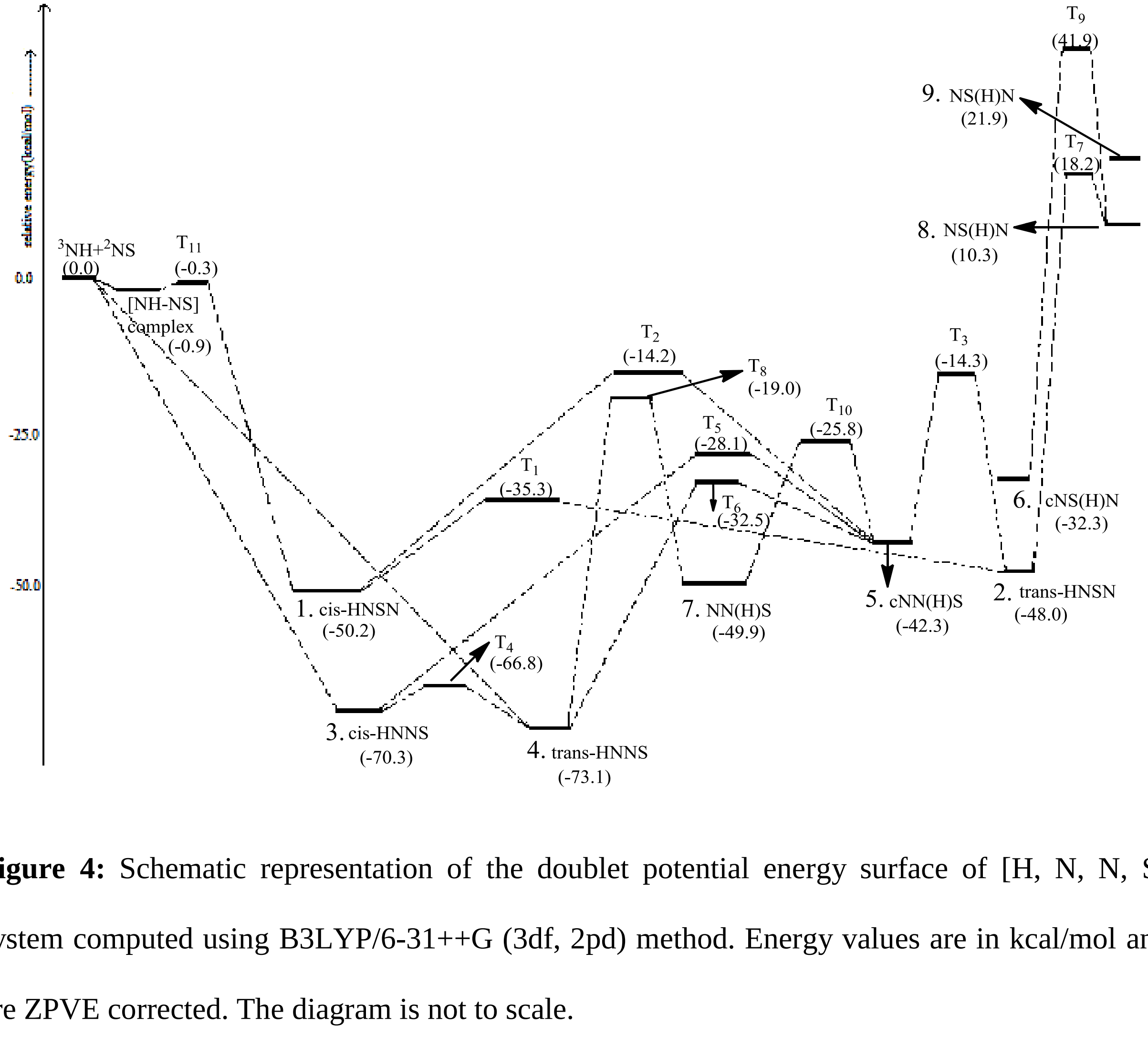

Figure 4: Schematic representation of the doublet potential energy surface of [H, N, N, S] system computed using B3LYP/6-31++G (3df, 2pd) method. Energy values are in kcal/mol and are ZPVE corrected. The diagram is not to scale.

Analysis of the PES shows that formation of most of the isomers is exothermic in nature, except for the isomers 8 and 9. Formation of isomer 8 is endothermic in nature and is 10.3 kcal/mol higher in energy compared to the reactants, NH and NS. Similarly, formation of the isomer 9 is endothermic in nature and is 21.9 kcal/mol higher in energy compared to the reactants, NH and NS. Instabilities for these two isomers might be arising due to their hyper-valent nature of the S-atoms in their structures. Moreover there are no direct paths for the formation of these two isomers, rather isomers 8 and 9 are coming from isomer 2 and 6 respectively, through very high energy isomerization barriers. Analysis of the relative energies of the other seven isomers shows that, isomer 4 which is the trans-HNNS is the most stable isomer (73.1 kcal/mol stable than the reactants, NH and NS), whereas the cis-HNNS (isomer 3) is only 2.8 kcal/mol higher in energy compared to this trans- isomer. Next set of isomers in view of stability are isomers 1, 2 and 7, which have almost equal stabilities, and are energetically above the isomers 3 and 4 (isomer 1, 2 and 7 are 50.2 kcal/mol, 48.0 kcal/mol and 49.9 kcal/mol stable respectively compared to the reactants, NH and NS). In terms of stability then comes isomer 5 and after that isomer 6. Isomer 5 is 42.3 kcal/mol and isomer 6 is 32.3 kcal/mol stable compared to the reactants, NH and NS. Thus, one can say that among the seven isomers, which can be formed exothermically from the reaction of NH and SN, isomer 4 is the most stable one and isomer 6 is the least stable. MP2 method also predicts similar order in terms of the stabilities of these isomers like that of the B3LYP method. Only in the case of isomer 9, which is endothermic comparted to the reactants, B3LYP method predicts it to be 21.9 kcal/mol higher and MP2 method predicts it to be 122.3 kcal/mol higher in energy compared to reactants (MP2 method predicts isomer 9 to be an exceptionally unstable isomer).

As discussed in the previous section, inclusion of the dispersion forces as well as long-range interactions into the DFT method showed that the complex is 1.5 kcal/mol stable than the reactants (BSSE corrections calculated for the complex was found to be very small; around 0.3 kcal/mol), and at the same time the TS (T_{11}) is 0.7 kcal/mol above the complex (almost 0.8 kcal/mol lower compared to the reactants). After inclusion of the dispersion forces and long-range interactions into the DFT method, this is the only reaction transition state we were able to locate. Once the isomers are formed, isomerization from one to other can happen under suitable conditions. After the formation of the isomer 3, it can either undergo a cis-trans isomerization process through T_4 to give the most stable isomer 4 (the barrier for this to happen is 3.5 kcal/mol), or it can isomerize to isomer 5 through T_5 (large barrier height of 42.2 kcal/mol). Now the isomer 5 can further isomerize in four different ways to give isomers 4, 1, 2 and 7, through transition states T_6, T_2, T_3 and T_{10}, respectively. The respective barrier heights for these four transition states T_6, T_2, T_3 and T_{10} from isomer 5 are 9.8 kcal/mol, 28.1 kcal/mol, 28.0 kcal/mol and 16.5 kcal/mol. Similarly, after the formation of 4, though there are one cis-trans isomerization and two other isomerization pathways, all of them are endothermic in nature. Now, after the formation of isomer 1, it can either undergo a cis-trans isomerization pathway through T_1 to give isomer 2, or it can isomerize to isomer 5 through T_2, and both the transformations are endothermic in nature. Besides some exceptions, in most of the cases B3LYP and MP2 methods predict similar kind of behaviour in the PES. MP2 method predicts T_2 barrier is very large (+7.7 kcal/mol in MP2 and -14.2 kcal/mol B3LYP methods compared to the reactants HS and NS). Similarly, MP2 method also predicts the T_5 barrier to be a large barrier (-8.5 kcal/mol for MP2 method and -28.1 kcal/mol for B3LYP methods). On the other side, MP2 method predicts T_7 to be a slightly lower barrier (10.0 kcal/mol for MP2 method and 18.2 kcal/mol for B3LYP method), T_9 to be a slightly larger barrier (54.7 kcal/mol for MP2 method and 41.9 kcal/mol for B3LYP method) and T_{10} to be a large barrier (-5.6 kcal/mol in MP2 method and -25.8 kcal/mol in B3LYP method).

3.4. Formation of molecular nitrogen (N_2) and SH:

Two important dissociation transition states T_{12} and T_{13} leading to the formation of N_2 + SH have been located in the PES. Analysis of T_{12} and T_{13} shows that they represent the dissociation channels from the isomers 3 and 5, respectively. Analysis of the PES shows that isomers 3-7, all of them have the characteristic N-N linkage, and have the potential to form the N_2 molecule, but we were able to locate only these two dissociation transition states. The complete paths leading to the formation of N_2 + SH, starting from the reactants, NH and NS, for these two cases are shown in Figure 5. As discussed in the introduction, till-date all the proposed reactions paths for the formation of N_2 in the interstellar medium starts with the interaction of atomic nitrogen (N) with other molecules, which at the end gives N_2 after multiple steps[11,21]. In this work an attempt has been made to explore the possibility of N_2 formation in this reaction PES. Similar reaction surface related to the reaction between NH and NO has also been extensively studied earlier and all of them indicate the formation of N_2+OH as one of the channels[28-38]. A comparison of our results for NH + NS reaction surface has also been made with the NH + OH reaction surface.

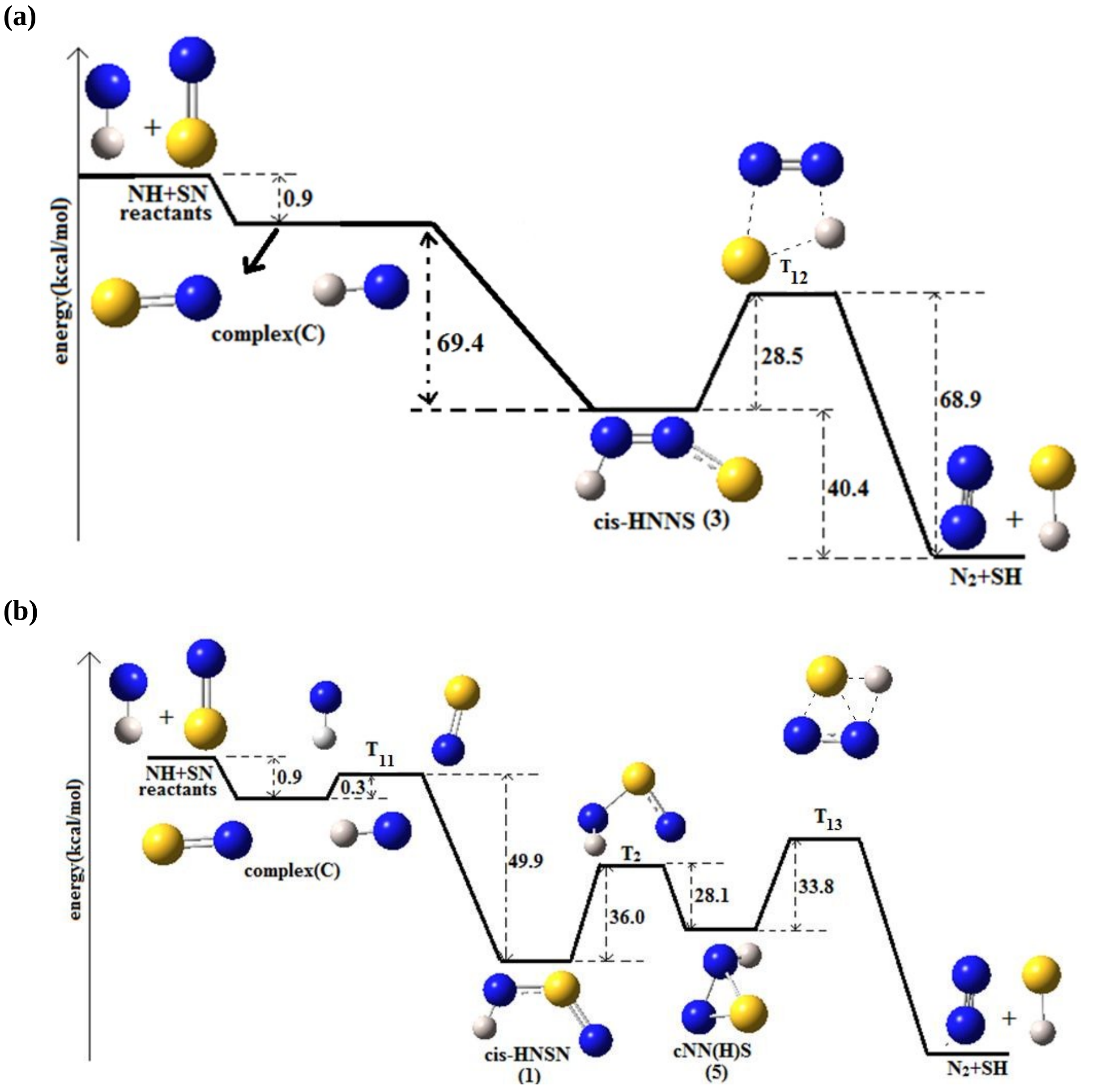

Figure 5: **(a)** Dissociation channel leading to the formation of N_2 + SH, from the reaction of HN + NS, through the isomer 3. **(b)** Dissociation channel leading to the formation of N_2 + SH, from the reaction of HN + NS, through isomer 5. B3LYP/6-31++G(3df,2pd) energy values shown in the diagrams are in kcal/mol and are ZPVE corrected. The diagram is not to scale.

Figure 5 (a) shows that the reaction of HN + NS leads directly to the isomer 3 (this reaction proceeds without any potential barrier as predicted by the wB97XD method, which includes the corrections due to dispersion forces and long range interactions), which then dissociates to give N_2 and SH, over the transition state, T_{12}. Isomer 3 undergoes a dissociation through a barrier height of 28.5 kcal/mol and it can also be found that products N_2 + SH is 40.1 kcal/mol more stable than isomer 3. This indicates that formation of N_2 + SH from isomer 3 is highly exothermic in nature. Similar to this, the PES of HN + NO reaction surface leading to the formation of N_2 + OH shows that, both the reactants first react to form a stable cis-isomer of HNNO (like the isomer 3 in our case), and this transformation goes through a reasonably small barrier. HNNO then dissociates through a reasonably large barrier to give the products N_2 + OH (in our case from isomer 3 to N_2+SH goes through the barrier of 28.5 kcal/mol high)[31,36,38]. This indicates that the PESs for the reactions HN + NO and NH + NS are showing almost similar kind of behaviour[31,36,38]. Unlike the NH + NO reaction surface, which shows only one reaction channel leading to the formation of N_2 + OH, in our case we were able to locate another reaction channel from the reaction of NH + NS leading to the formation of N_2 + SH, and is shown in Figure 5 (b)[36]. The path shows that reaction between NH and NS first leads to the formation of isomer 1, which then isomerises to isomer 5. Isomerization step from isomer 1 to isomer 5 is endothermic in nature and passes through a large barrier height of 36.0 kcal/mol. Isomer 5 then dissociates through transition state, T_{13} to give N_2+SH and the barrier height is 33.8 kcal/mol compared to isomer 5. Unlike the previous case [Figure 5(a)] where all the steps in the reaction path were exothermic, in this case the isomerization step from isomer 1 to 5 is endothermic in nature. Though overall reaction channel is exothermic in nature, this step some time might create problem in extremely low temperature conditions.

3.4.1. Possibility of formation of N_2 and SH in interstellar conditions:

In the interstellar medium (ISM), hot-cores are the dense and warm regions consisting of gases and dusts, which are rich in exotic gas chemistries[54,55]. High temperature in those hot-cores (around 200K - 1000K) can facilitate most of the high barrier reactions[54]. Powered by the high energies of the hot-cores[54], both the reactions discussed above, can be able to surmount the barriers present in their paths leading to the formation of N_2 + SH starting from the HN + NS. Thus the formation of N_2 in hot-core regimes of the ISM through both the reaction channels can be considered as quite affirmative.

Reactions in the cold-cores or cold interstellar clouds in the ISM (where the temperature is quite low and even close to 10 K) are quite complicated[56]. It is generally believed that, barriers if present in the reaction paths, they act as bottlenecks to any reactions at these temperature conditions. The only way such a reaction will be possible at this extreme low temperature, if there is an operative tunnelling mechanism[57]. To analyse the possibility of any tunnelling mechanism, our first check was the imaginary frequencies of the dissociation transition states T_{12} and T_{13}. It is known that, one can have some qualitative information about the width of a barrier from its imaginary frequency[37], where the lower value of the TS imaginary frequency is associated with a gentler and broader barrier, and the higher value of imaginary frequency corresponds to a sharper and narrower barrier[57]. A sharper and narrower barrier facilitates the tunnelling to happen, if the transition state exhibits a prominent proton dynamics[57,58].

Analysis of the imaginary frequency related to transition state T_{12} shows that it is quite large (1904i cm^{-1}) and thus indicates a sharper and narrower barrier for the dissociation. Also, analysis of the displacement vectors of the vibration related to imaginary frequency indicates a prominent hydrogen dynamics. Such a case seems to be highly favourable for the dissociation to happen with tunnelling playing the significant role in extremely low temperature conditions prevailing in the interstellar medium. Thus, one can say that, though the dissociation reaction from isomer 3 to N_2 + SH is having a very large barrier, the prominent effect of tunnelling will be able to make this reaction feasible and thus the formation of the N_2 in the low temperature regime of the ISM is very much probable. Similarly, analysis of the imaginary frequency related to T_{13} (1514i cm^{-1}) shows that dissociation from isomer 5 to N_2 + SH is also a sharper and narrower barrier, and also the displacement vectors of the vibration related to imaginary frequency indicates a prominent hydrogen dynamics. Thus effect of tunnelling can also be expected in this dissociation process form isomer 5 to N_2 + SH. But owing to the endothermic nature of the penultimate isomerization process (isomerization form isomer 1 to 5), feasibility of such dissociation in extreme low temperature conditions prevailing in the interstellar medium is at this time can be considered as doubtful, until it is being verified by further experimental investigations or theoretical calculations related to kinetics of this reaction. Thus we can say at least channel 1 [Figure 5(a)] is a definite path for the formation of N_2 in the ISM, in the divergent temperature conditions existing in the ISM (proving its universality nature), and probably can be considered as one of the contributing channel while accounting for the total estimates of the N_2 in the ISM. Moreover in the competition between the two reactions shown in Figure 5, formation of N_2 through isomer 3 will be the dominant channel.

Other interesting thing we can infer here is that besides the formation of N_2 in the low temperature regions of ISM, our study also shows the possible formation of the other fragment, SH in equal molar ratio to that of the N_2. As mentioned by Yamamura et al.[59] the existence of SH is doubtful in the very low temperature regions of the ISM, but on the other hand the present study strongly supports the possible existence of SH in the colder regions of ISM. Importance of this simple fragment SH (mercapto radical) is quite evident from the fact that the entire instrument, GREAT (**G**erman **Re**ceiver for **A**stronomy at **T**erahertz Frequencies) of the SOFIA (the **S**tratospheric **O**bservatory **f**or **I**nfrared **A**stronomy) a joint US/German project, has been dedicated to find it[60]. One of the reasons as specified by Neufeld and his co-workers is that, as SH is formed at certain temperature, especially possible in those parts of the interstellar clouds which are heated up to much higher temperatures.[61] But, interestingly our results show that this simple radical, SH can even be formed at extremely low temperature conditions from the reaction of HN and SN, which are readily available in the clod interstellar clouds.

4. Conclusions:

Using computational calculations we have carried out the complete PES analysis of the reaction between the fragments NH and NS, which are already detected in interstellar medium. The PES shows that the association reaction between the two fragments is highly exothermic in nature, which indicates the possibility of formation of many stable isomers from this reaction. Owing to the availability of the both NH and NS in the ISM and highly exothermic nature of the reaction surface, we suggest that the species like HNNS and HNNS can possibly be detected in the interstellar medium in future. Analysis of the dissociation channels indicated one of the important dissociation paths leading to the formation of N_2 from the isomer, *cis*-HNNS. We have shown that this dissociation is highly feasible due to the highly exothermic nature of the reaction path and also at the same time cited how tunnelling effect will make this reaction to produce N_2 in the extremely low temperature conditions prevailing in the interstellar medium. We have proposed for the first time that the formation of N_2 from the association of HN and NS (rather than the earlier considerations where interstellar formation of N_2 were mostly considered mostly in multi stepped processes staring with atomic N), and also argued that the similar reaction of HN + NO (based on the earlier works related to this reaction) can also be considered as a channel for the interstellar formation of N_2. Based on our discussion we have proposed that the reaction between NH and NS (and also reaction between NH and NO) can probably be considered as the contributing secondary channel(s) while accounting for the total estimates of the N_2 in the interstellar medium as well as the elemental nitrogen partitioning in the ISM. On the other hand the dissociation reaction leading to the formation of N_2 indicates the formation of another interesting radical SH. It is proposed that the formation of SH through the reaction of HN and NS is possible also in the cold interstellar clouds exhibiting extremely low temperature conditions.

Acknowledgements: The authors like to thank University of Johannesburg for the support. SS thanks the NRF, South Africa for incentive funding. PB thanks University of Johannesburg for the PhD bursary. ZPN thanks NRF, South Africa for PhD bursary.

Supporting Information: Table S1 shows the comparison of the relative energies of various isomers and transition states using B3LYP/aug-cc-pvtz, MP2/6-31++G(3df,2pd) and G3B3 methods. Table S2 shows the harmonic frequencies and their IR intensities of the isomers calculated from B3LYP/6-31++G(3df,2pd) and MP2/6-31++G(3df,2pd) methods. Similarly, the harmonic frequencies and their IR intensities of the transition states calculated from B3LYP/6-31++G(3df,2pd) and MP2/6-31++G(3df,2pd) methods are shown in Table S3. Then various possible fragments (Figure S1) and their possible dissociation paths have been provided in the section with heading as fragments. At the end MP2/6-31++G(3df,2pd) optimized geometries in Cartesian coordinates of all the stationary points in the PES have been provided. Optimized geometries of the complex and some of the transition states obtained at wB97XD method are also provided in the supporting information.

References:

1. For a complete up-to-date list of interstellar and circumstellar molecules, see http://www.astrochymist.org/astrochymist_ism.html and http://www.astro.uni-koeln.de/cdms/molecules.

2. T. P. Snow, B. J. McCall, *Ann. Rev.Astron. Astrophys.*,2006, **44**, 367–414.

3. S. Thorwirth, V. Lattanzi, L. A. Muck, D. T. Halfen, S. Brunken, C. A. Gottlieb, P. Thaddeus, L. M. Ziurys, J. Gauss, M. C. McCarthy , *Proceedings of The International Astronomical Union*, 2011, **280**.

4. Eric Herbst, E. F. van Dishoeck, *Annual Review of Astronomy and Astrophysics*, 2009, **47**, 427-480.

5. A. P. C. MANN & D. A. WILLIAMS, *Nature* **283**, 721 - 725 (21 February 1980); doi:10.1038/283721a0

6. W. J. Maciel, in "*Astrophysics of the Interstellar Medium*" 2012, 215-237.

7. J. Tennyson, "Molecules in Space" in "*Handbook of Molecular Physics and Quantum Chemistry*" Eds., S. Wilson, 2003, **3**, 356-369.

8. K. M. Menten, F. Wyrowski, "Molecules Detected in Interstellar Space" in "*Interstellar Molecules*" 2011, **241**, 27-42.

9. K. M. T. Yamada, G. Winnewisser, "List of Molecules Observed in Interstellar Space" in "*Interstellar Molecules*", 2011, **241**, 219-223.

10. H. S. P. Müller, F. Schlöder, S. Thorwirth, G. Winnewisser, "The Cologne Database for Molecular Spectroscopy, CDMS " in "*The Dense Interstellar Medium in Galaxies*" 2004, **91**, 95-98

11. G. Pineau des Forets, E. Roueff, D. R. Flower, *Monthly Notices of the Royal Astronomical Society*, 1990, **244**, 668-674.

12. E. Herbst, E. F. van Dishoeck, *Annu. Rev. Astron. Astrophys.*, 2009, **47**, 427–480.

13. J. Lequeux, E. Roueff, *Physics Reports*, 1991, **200**, 241—299.

14. P. Hily-Blant, M. Walmsley, G. Pineau des Forets, D. Flower, *Astronomy & Astrophysics*, 2010, **513**, A41.

15. M. Larsson, W. Geppert, G. Nyman, *Reports on Progress in Physics*, 2012, **75**, 066901.

16. V. Wakelam, I. W. M. Smith, J. -C. Loison, D. Talbi, S. J. Klippenstein, A. Bergeat, W. D. Geppert, K. M. Hickson, http://arxiv.org/abs/1310.4350v1.

17. D. R. Flower, G. Pineau des Forets, C. M. Walmsley, *Astronomy & Astrophysics*, 2006, **456**, 215-223.

18. R. Le Gal, P. Hily-Blant, A. Faure, G. Pineau des Forêts, C. Rist, S. Maret, *Astronomy & Astrophysics*, 2014, **562**, A83.

19. J. B. Pickles, D. A. Williams, *Astrophysics and Space science*, 1977, **52**, 453-478.

20. Z. –C. Wang, C. A. Cole, N. J. Demarais, T. P. Snow, V. M. Bierbaum, *J. Am. Chem. Soc.*, 2015, **137**, 10700–10709.

21. J. Daranlot, U. Hincelin, A. Bergeat, M. Costes, J. –C. Loison, V. Wakelam, K. M. Hickson, Proc. Natl. Acad. Sci., 2012, **109**, 10233-10238.

22. D. C. Knauth, B. –G. Andersson, S. R. McCandliss, H. Warren Moos, *Nature*, 2004, **429**, 636–638.

23. P. Hily-Blant, S. Maret, A. Bacmann, S. Bottinelli, B. Parise, E. Caux, A. Faure, E. Bergin, G. A. Blake, A. Castets, C. Ceccarelli, J. Cernicharo, A. Coutens, N. Crimier, K. Demyk, C. Dominik, M. Gerin, P. Hennebelle, T. Henning, C. Kahane, A. Klotz, G. Melnick, L. Pagani, P. Schilke, C. Vastel, V. Wakelam, A. Walters, A. Baudry, T. Bell, M. Benedettini, A. Boogert, S. Cabrit, P. Caselli, C. Codella, C. Comito, P. Encrenaz, E. Falgarone, A. Fuente, P. F. Goldsmith, F. Helmich, E. Herbst, T. Jacq, M. Kama, W. Langer, B. Lefloch, D. Lis, S. Lord, A. Lorenzani, D. Neufeld, B. Nisini, S. Pacheco, T. Phillips, M. Salez, P. Saraceno, K. Schuster, X. Tielens, F.

van der Tak, M. H. D. van der Wiel, S. Viti, F. Wyrowski, H. Yorke, *Astronomy & Astrophysics*, 2010, **521**, L52.

24. M. Womack, L. M. Ziurys, S. Wyckoff, *Astrophys. J*, 1992, **387**, 417-429.

25. S. Maret, E. A. Bergin, C. J. Lada, *Nature*, 2006, **442**, 425-427.

26. M. Womack, L. M. Ziurys, S. Wyckoff, *Astrophys. J.*, 1992 **393**,188-192.

27. D. M. Meyer, J. A. Cardelli, U. J. Sofia, *Astrophys. J.*, 1997, **490**, L103-L106.

28. K. A. Peterson, J. S. Francisco, *J. Chem. Phys.*, 2011, **134**,084308.

29. M. C. McCarthy, O. Martinez Jr., K. N. Crabtree, V. Lattanzi, S. E. Novick, S. Thorwirth, *J. Phys. Chem. A*, 2013, **117**, 9968–9974.

30. X. Huang, R. C. Fortenberry, T. J. Lee, *J. Chem. Phys.*, 2013, **139**, 084313.

31. K. S. Bradley, P. McCabe, G. C. Schatz, S. P. Walch, *J. Chem. Phys.*, 1995, **102**, 6696.

32. M. Simonson, K. S. Bradley, G. C. Schatz, *Chem. Phys. Lett.*, 1995, **244**, 19-26.

33. H. Szichman, M. Baer, *J. Chem. Phys.*, 1996, **105**, 10380-10386.

34. A. M. Mebel, M. C. Lin, *Int. Rev. Phys. Chem.*, 1997, **16**, 249-266.

35. P. Marshall, A. Fontijin, C. F. Melius, *J. Chem. Phys.*, 1987, **86**, 5540.

36. S. P. Walch, *J. Chem. Phys.*, 1993, **98**, 1170.

37. J. L. Durant, *J. Phys. Chem.*, 1994, **98**, 518.

38. S. Kristyan, M. C. Lin, *Chem. Phys. Lett.*, 1998, **297**, 200-204.

39. D. M. Meyer, K. C. Roth, *Astrophys. J.*, 1991, **376**, L49–L52.

40. R. Wagenblast, D. A. Williams, T. J. Millar, L. A. M. Nejad, *Monthly Notices of the Royal Astronomical Society*, 1993, **260**, 420-424.

41. C. A. Gottlieb, J. A. Ball, E. W. Gottlieb, C. J. Lada, H. Penfield, *Astrophys. J.*, 1975, **200**, L147-L149.

42. D. McGonagle, W. M. Irvine, M. Ohishi, *Astrophys. J.*, 1994, **422**, 621-625.

43. D. McGonagle, W. M. Irvine, *Astrophys J.*, 1997, **477**, 711-721.

44. M. J. Frisch, G. W. Trucks, H. B. Schlegel, G. E. Scuseria, M. A. Robb, J. R. Cheeseman, G. Scalmani, V. Barone, B. Mennucci, G. A. Petersson, H. Nakatsuji, M. Caricato, X. Li, H. P. Hratchian, A. F. Izmaylov, J. Bloino, G. Zheng, J. L. Sonnenberg, M. Hada, M. Ehara, K. Toyota, R. Fukuda, J. Hasegawa, M. Ishida, T. Nakajima, Y. Honda, O. Kitao, H. Nakai, T. Vreven, J. A. Montgomery, Jr., J. E. Peralta, F. Ogliaro, M. Bearpark, J. J. Heyd, E. Brothers, K. N. Kudin, V. N. Staroverov, R. Kobayashi, J. Normand, K. Raghavachari, A. Rendell, J. C. Burant, S. S. Iyengar, J. Tomasi, M. Cossi, N. Rega, J. M. Millam, M. Klene, J. E. Knox, J. B. Cross, V. Bakken, C. Adamo, J. Jaramillo, R. Gomperts, R. E. Stratmann, O. Yazyev, A. J. Austin, R. Cammi, C. Pomelli, J. W. Ochterski, R. L. Martin, K. Morokuma, V. G. Zakrzewski, G. A. Voth, P. Salvador, J. J. Dannenberg, S. Dapprich, A. D. Daniels, Ö. Farkas, J. B. Foresman, J. V. Ortiz, J. Cioslowski, and D. J. Fox, Gaussian 09, Gaussian, Inc., Wallingford CT, 2009.

45. A. D. Becke, *J. Chem. Phys.*, 1993, **98,** 5648-5652.

46. C. Lee, W. Yang, R. G. Parr, *Phys. Rev. B*, 1988, **37**, 785-789.

47. J. A. Pople, R. K. Nesbet, *J. Chem. Phys.*, 1954, **22**, 571-72.

48. M. J. Frisch, M. Head-Gordon, J. A. Pople, *Chem. Phys. Lett.*, 1990, **166**, 275-280.

49. M. J. Frisch, M. Head-Gordon, J. A. Pople, *Chem. Phys. Lett.*, 1990, **166**, 281-289.

50. S. F. Boys, F. Bernardi, *Mol. Phys.*, 1970, **19**, 553.

51. H. P. Hratchian, H. B. Schlegel, *J. Chem. Phys.*, 2004, **120**, 9918-9924.

52. A. G. Baboul, L. A. Curtiss, P. C. Redfern, K. Raghavachari, *J. Chem. Phys.*, 1999, **110**, 7650-7657.

53. J. -D. Chai, M. Head-Gordon, *Phys. Chem. Chem. Phys.*, 2008, **10**, 6615-6620.

54. R. T. Garrod, S. L. W. Weaver, *Chem. Rev.*, 2013, **113**, 8939–8960.

55. E. F. van Dishoeck, G. A. Blake, *Ann. Rev. Astron. Astrophys.*, 1998, **36**, 317-368.

56. E. Herbst, *Chem. Soc. Rev.*, 2001, **30**, 168-176.

57. R. J. Shannon, M. A. Blitz, A. Goddard, D. E. Heard, *Nat. Chem.*, 2013, **5**, 745–749.

58. I. W. M. Smith, A. R. Ravishankara, *J. Phys. Chem. A*, 2002, **106**, 4798-4807.

59. I. Yamamura, K. Kawaguchi, S. T. Ridgway, *Astrophys. J.*, 2000, **528**, L33-L36.

60. A. Krabbe, D. Mehlert, H.-P. Roser, C. Scorza, *Eur. J. Phys.*, 2013, **34**, S161-S177.

61. D. A. Neufeld, E. Falgarone, M. Gerin, B. Godard, E. Herbst, G. Pineau des Forets, A. I. Vasyunin, R. Gusten, H. Wiesemeyer, O. Ricken, *Astronomy and Astrophysics*, 2012, **542**, L6.

TOC Graphics

Reaction between HN and SN: A possible channel for the interstellar formation of N_2 and SH in the cold interstellar clouds.

Authors: Priya Bhasi, Zanele P. Nhlabatsi, Sanyasi Sitha*

Department of Chemistry, University of Johannesburg, PO Box 524, Auckland Park, Johannesburg, South Africa 2006.

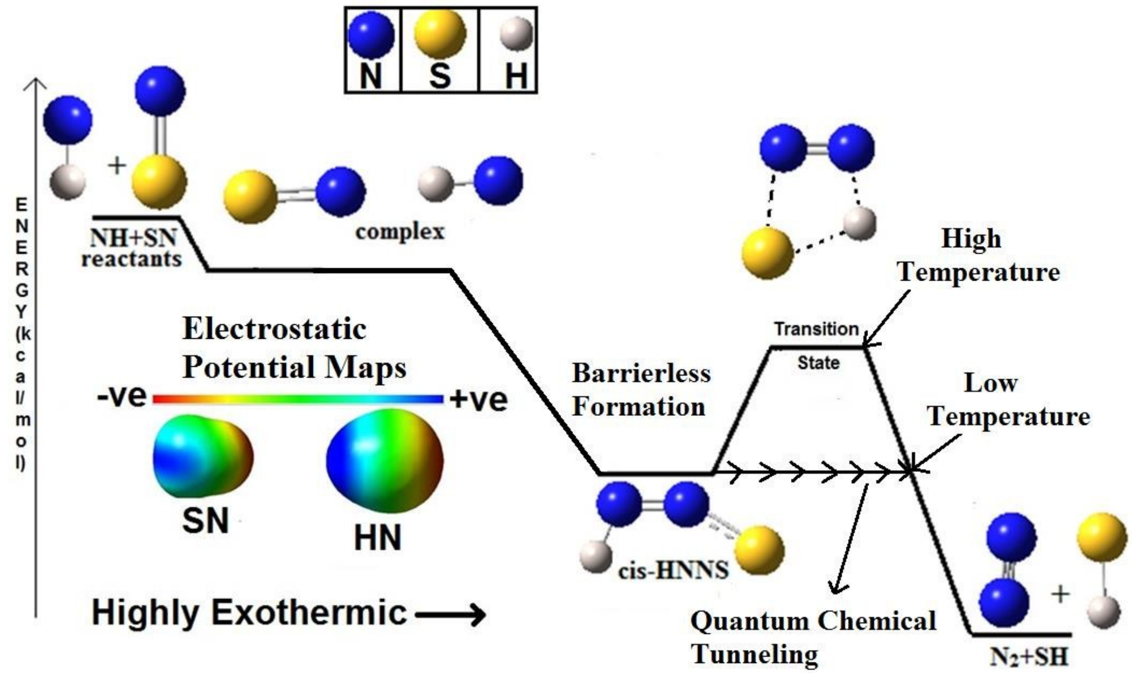

Computational study of the reaction between HN and NS shows the formation of N_2 and SH in the cold interstellar clouds.